ChemComm

Tetrahedral Iron Featuring an Appended Lewis Acid: Distinct Pathways for the Reduction of Hydroxylamine and Hydrazine

Journal:	*ChemComm*
Manuscript ID	CC-COM-07-2019-005720.R1
Article Type:	Communication

COMMUNICATION

Tetrahedral Iron Featuring an Appended Lewis Acid: Distinct Pathways for the Reduction of Hydroxylamine and Hydrazine

Received 00th January 20xx,
Accepted 00th January 20xx

DOI: 10.1039/x0xx00000x

John J. Kiernicki,[a] Emily E. Norwine,[a] Mattias Zeller,[b] and Nathaniel K. Szymczak*[a]

We present the preparation of a nitrogen-based bidentate ligand featuring an appended boron Lewis acid as well as its tetrahedral Fe^{2+} and Zn^{2+} complexes. These complexes act as platforms for hydrazine and hydroxylamine capture and reduction chemistry.

The unparalleled ability of nitrogenase to reduce small molecule substrates through series of H^+/e^- transfer reactions remains unmatched by synthetic chemists. Spectroscopic, computational, biochemical, and X-ray methods have greatly improved our knowledge regarding details of the reduction pathway of the ubiquitous nitrogenase substrate, N_2, although critical, unanswered questions still remain that are needed to assemble a full mechanistic model or scheme.[1] A key step proposed for NH_3 production is the cleavage of the N-N bond of a hydrazine intermediate by low-coordinate, high-spin iron.[1f] In analogy, the final reduction sequence of nitrite, an established nitrogenase substrate,[2] has also been proposed to follow a pathway whereby cleavage of the N-O bond of hydroxylamine (NH_2OH) affords an Fe-NH_2.[3, 4]

In addition to the primary coordination environment, the nitrogenase active site features acidic groups near the N_2 binding site that may function to facilitate binding, activation, and/or N-N bond scission.[1a] Our group is working to evaluate how the precise structural, electronic, and cooperative modes in the secondary coordination sphere can be used to regulate reactivity.[5] Among the substrates whose reactivity can be controlled by secondary sphere Lewis acids is hydrazine, an intermediate proposed during N_2 reduction.[6] The paralleled reduction sequences of N_2H_4 and NH_2OH afford an opportunity to probe mechanistic hypotheses regarding the role(s) of a Lewis acidic group for controlled bond scission at a low coordinate metal.[1a, 1f] Herein, we report the synthesis of tetrahedral iron complexes that contain a flexible appended boron Lewis acid and their reactivity toward hydrazine and hydroxylamine.

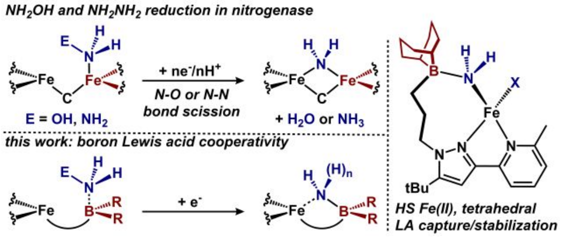

Figure 1. Top left: proposed reduction pathway for N_2 and NO_2^- by nitrogenase leading to a common amido intermediate. Bottom right: our approach to probe N-O or N-N bond scission with boron Lewis acids. Right: Lewis acid-appended platform used in this study.

To establish a tetrahedral platform suitable for evaluating N-N and N-O bond scission, we targeted a bidentate variant of the tridentate pincer, 2,6-bis(5-*tert*-butyl-1(propyl-BBN)-pyrazol-3-yl)pyridine (BBN = 9-borabicyclo[3.3.1]nonyl), that we previously reported.[6b] The ligand, 2-(1-allyl-5-(*tert*-butyl)-1H-pyrazol-3-yl)-6-methylpyridine ($^{allyl}NN^{tBu}$), was synthesized in one step from 2-(5-(*tert*-butyl)-1H-pyrazol-3-yl)-6-methylpyridine[7] and metalated with FeX_2 (X = Cl, Br) in CH_2Cl_2 to afford orange ($^{allyl}NN^{tBu}$)FeX_2 (**1-X**; Fig. 1). We pursued post-metalation hydroboration to install the Lewis acidic borane unit, a strategy that overcomes pre-metalation acid/base incompatibilities.[6c, 8] Stirring a THF solution of **1-X** with 9-BBN at room temperature enabled anti-Markovnikov addition to the allylic moiety, affording yellow ($^{BBN}NN^{tBu}$)FeX_2 (**2-X**; Fig. 2) in 87-97% yield.

Complexes **1-X** and **2-X** are high-spin (μ_{eff} values range 5.4-5.6 μB; 25 °C, THF) C_s symmetric paramagnets with ^1H NMR resonances ranging between -27 and +53 ppm. The molecular structures of **1-X** and **2-X** were established using single crystal X-ray diffraction (XRD). Each complex displays a near tetrahedral coordination environment at iron (τ_4 range 0.85-0.88)[9] with Fe-$N_{pyridine}$ (ave. = 2.133 Å) and Fe-$N_{pyrazole}$ (ave. = 2.075 Å) bond distances minimally perturbed by hydroboration (Fig. 2, Table S20). Complexes **2-X** contain trialkylborane pendent groups with ΣB_α values near 360°, consistent with

---

[a] University of Michigan, 930 N. University, Ann Arbor, MI 48109, USA. E-mail: nszym@umich.edu

[b] H. C. Brown Laboratory, Purdue University, 560 Oval Dr, West Lafayette, IN 47907, USA

Electronic Supplementary Information (ESI) available. CCDC numbers. For ESI and crystallographic data in CIF see DOI: 10.1039/x0xx00000x unquenched Lewis acids. Voltammetry experiments (0.2 M $[Bu_4N][PF_6]$, THF) were employed to assess electronic changes imparted by hydroboration. The reduction wave of **1-Br** (-2.05 V; vs Fc/Fc^+) is shifted negatively (70 mV) upon hydroboration to **2-Br**, consistent with modest electronic alteration of the metal centre.[10]

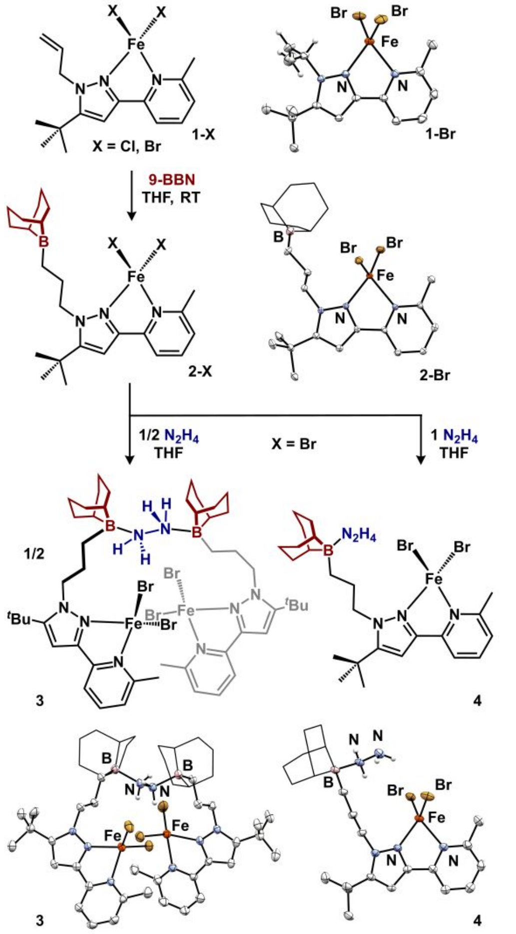

Figure 2. Late-stage hydroboration to form **2-X** and hydrazine capture to form **3** and **4**. Molecular structures of **1-Br**, **2-Br**, **3**, and **4** displayed with 50% probability ellipsoids. H-atoms not attached to hydrazine or allyl substituents are omitted for clarity.

To assess acid/base interactions accessible within the secondary coordination sphere, **2-Br** was treated with either ½ equiv. or 1 equiv. of N_2H_4 and analysed. Data obtained from both IR and ^1H NMR spectroscopies suggest two distinct products are formed. To clarify the molecular structures, crystals from each reaction were analysed by XRD. The monomeric 1:1 adduct, $(^{BBN}NN^{tBu})FeBr_2(N_2H_4)$ (**4**), was the product of equimolar addition, while $[(^{BBN}NN^{tBu})FeBr_2]_2(N_2H_4)$ (**3**), a dimeric species, was the product of substoichiometric addition (Fig. 2, bottom). The monomeric adduct, **4**, contains a pyramidalized trialkylborane (ΣB_α = 321.79(14)°) that interacts with hydrazine (B-N = 1.646(2) Å) while both $-NH_2$ fragments participate in weak intramolecular hydrogen bonding interactions with a bromide ligand ($Br\text{-}N_{ave}$ = 3.607 Å).[11] In complex **3**, both hydrazine lone-pairs are quenched by boranes of adjacent molecules with a slightly weaker interaction ($B\text{-}N_{ave}$ = 1.687 Å).[12] A recent related example found that a rigid diborane binding pocket was selective for binding only a single equivalent of N_2H_4.[13] Because **4** can be formed from **3** + N_2H_4, *flexibility* of the appended alkyl borane is a key factor that enables B-N bond equilibration and monomer/dimer speciation. Compared to **2-Br**, the primary coordination sphere bond metrics of both **3** and **4** are unperturbed, and notably, do not display any short NH_2-Fe contacts, indicating that there is no interaction of N_2H_4 with the iron centre.

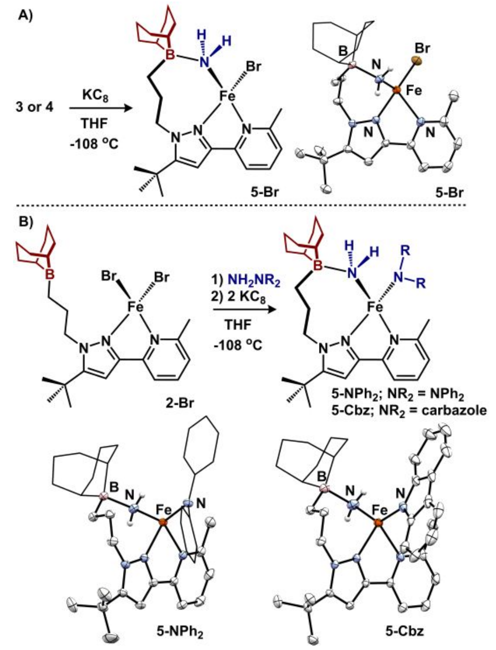

Figure 3. Top: reduction of **3** and **4** to form **5-Br**. Bottom: reductive cleavage of 1,1-disubstituted hydrazines to form **5-NPh₂** and **5-Cbz**. For both **3** and **4**, 2 equiv. KC_8 were used. Molecular structures are displayed with 50% probability ellipsoids. H-atoms not attached to amido substituents are omitted for clarity.

The secondary coordination sphere Lewis acids in complexes **3** and **4** dictate hydrazine binding *independent* of the metal centre. We pursued N–N bond scission to investigate the role of 2° interactions in subsequent redox reactions. To probe the ability of **3** and **4** to be reduced, each species was interrogated electrochemically. Voltammetry (0.2 M $[Bu_4N][PF_6]$, THF) experiments revealed both complexes exhibit a quasi-reversible reduction event near -2.06 V (vs. Fc/Fc^+).[14] To chemically effect this reduction, freshly thawed THF solutions of each were treated with two equiv. of KC_8. Following workup, a common yellow species assigned as $(^{BBN}NN^{tBu})FeBr(NH_2)$ (**5-Br**) was obtained. NMR and IR spectroscopies revealed C_1 symmetry, with two N-H vibrations (3328, 3264 cm^{-1}), respectively (see ESI).

N-N bond cleavage of hydrazines can occur either through uneconomical disproportionation which produces a maximum of 1.33 equiv. NH_3 per equiv. N_2H_4,[15] or homolytic scission (up to 2 equiv. NH_3).[6b, 16] To gain insight into the operative reduction pathway by **3** or **4**, we assessed the reaction stoichiometry when reducing N_2H_4 to NH_2^- by quenching crude mixtures with HCl and quantifying the amount of NH_4^+.[17] Addition of 2 equiv. of KC_8 to a freshly thawed THF solution of **4** followed by HCl produced NH_4^+ in 75% yield (1.49 equiv.; see Table S2 for quantification studies). Repeating the reaction with **3** afforded a similar result (68% yield; 1.36 equiv. NH_4^+).[18] Both results are consistent with *homolytic* N-N bond scission as the dominant reduction pathway.

We evaluated a series of control complexes to further clarify the roles of both the iron centre and the appended Lewis acid. We synthesized zinc analogues of **3** and **4** using identical conditions and evaluated their reductive capabilities to cleave hydrazine. In contrast to the Fe complexes, the Zn analogues did not produce NH_4^+ upon reduction/quenching. These results confirm the requirement of a redox-active metal to promote stoichiometric cleavage of N_2H_4 into NH_2^- equivalents. To probe the role of the trialkylborane in this transformation, we replaced the $–(CH_2)_3$BBN portion of the ligand with an *n*-butyl substituent and metalated with $FeBr_2$ to afford $(^{butyl}NN^{tBu})FeBr_2$. Treating $(^{butyl}NN^{tBu})FeBr_2$ with one equiv. of N_2H_4 in THF afforded a white precipitate from the yellow solution. Analysis of the solution revealed both $(^{butyl}NN^{tBu})FeBr_2$ and uncoordinated $(^{butyl}NN^{tBu})$, suggesting either: 1) N_2H_4 is a more competent ligand than $(^{butyl}NN^{tBu})$, or 2) $(^{butyl}NN^{tBu})FeBr_2$ may be a N_2H_4 disproportionation catalyst. To probe the latter, a sealed reaction flask of $(^{butyl}NN^{tBu})FeBr_2$ and N_2H_4 was stirred for 30 min, then treated with HCl. No NH_4^+ was detected, suggesting N_2H_4 serves to outcompete the (pyrazolyl)pyridine ligand for Fe. Overall, the series of control complexes provide strong support that the boron Lewis acids in **3** and **4** function to temper the reactivity of hydrazine — positioning the substrate until an electron source is available to perform productive chemistry.

We hypothesized that reduction of **4** occurs with concomitant loss of insoluble KNH_2 and that the delivery of both amido fragments to the metal centre might be possible if using an organic hydrazine. To evaluate this possibility, **2-Br** was separately treated with 1,1-diphenylhydrazine and 1-aminocarbazole in THF followed by reduction with KC_8.[19] Each reaction yielded products with spectroscopic (^1H NMR, IR) features similar to **5-Br**, leading to their assignments as $(^{BBN}NN^{tBu})Fe(NH_2)(NPh_2)$ (**5-NPh$_2$**) and $(^{BBN}NN^{tBu})Fe(NH_2(CBz)$ (**5-Cbz**). Complexes **5** are all high-spin (μ_{eff} values range 4.8-5.1 μB; 25 °C, THF) and moderately stable with half-lives of *ca*. 16 hr in THF solution at room temperature. Identification of their molecular structures by XRD enabled metrical parameter comparisons between the three amidoborane complexes (Fig. 3, Table S22). Each is best described as tetrahedral (τ_4 values span 0.79-0.85) with a parent amido ligand ($–NH_2$) capped by the trialkylborane group. The B-NH_2 distances are identical across the series (1.632 Å) while the Fe-NH_2 distance varies slightly, depending on the nature of the other X-type ligand. **5-Br** displays the shortest Fe-NH_2 contact (2.0187(17) Å) while **5-NPh$_2$** displays the longest (2.0533(14) Å). Interestingly, the Fe-NPh_2 (1.9856(15) Å) and Fe-Cbz (1.9915(13) Å) bond distances are significantly shorter than their respective Fe-NH_2 counterparts, presumably due to a decrease in π-bonding imparted by quenching of the NH_2-lone pair by the borane.

N_2H_4 and NH_2OH have been proposed to be intermediates in the biological fixation of N_2 and NO_2^-, respectively. Subsequent reduction of both species have been demonstrated to share a common reduction pathway featuring an iron amido (NH_2^-).[3] In analogy to N_2H_4, disproportionation of NH_2OH has been shown to produce mixtures of NH_3, H_2O, and N_2O or N_2 in small molecule platforms.[20] We envisioned employing **2-Br** as a chemical probe for the formation of common intermediate(s) for both isostructural compounds, N_2H_4 and NH_2OH.

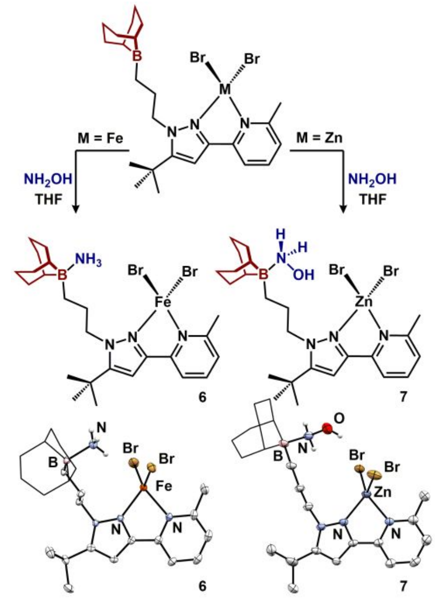

Figure 4. Left: Disproportionation of NH_2OH with **2-Br** to form **6**. Right: NH_2OH capture by zinc species to form **7**. Bottom: Molecular structures of **6** and **7** displayed with 50% probability ellipsoids. H-atoms not attached to heteroatoms are omitted for clarity.

Treating a THF solution of **2-Br** with a single equivalent of NH_2OH (50% v/v in H_2O) produced small quantities of a new material (*ca*. 20%) with predominantly starting material remaining. When the stoichiometry of NH_2OH was increased (6-8 equiv.), full consumption of **2-Br** occurred with formation of a new complex, $(^{BBN}NN^{tBu})FeBr_2(NH_3)$ (**6**) (Fig. 4). Note that **6** represents a common intermediate during the reduction of both N_2H_4 and NH_2OH because it can be formed by proton transfer to **5-Br** (see ESI).

The key difference between the **2-Br** mediated reduction of hydrazine and hydroxylamine is the source of electrons. Unlike N_2H_4, reduction of NH_2OH could occur via disproportionation to produce NH_3. To evaluate this hypothesis, the stoichiometric reaction was quenched with HCl: 0.25 +/- 0.03 equiv. NH_4^+ were produced. The addition of superstoichiometric quantities of NH_2OH to **2-Br** (5.56 mol%) produced 0.22 equiv. NH_4^+ per equiv. NH_2OH suggesting **2-Br** can function as a hydroxylamine disproportionation catalyst.[21] Hydroxylamine disproportionation is known to proceed via two distinct pathways that produce either N_2 or N_2O.[20] To test whether the N_2O production pathway was operative, we investigated the reaction headspace by IR spectroscopy and observed bands at 2236 and 2212 cm^{-1} that are diagnostic for N_2O (Fig. S50). These data suggest an active pathway for NH_2OH disproportionation in this system follows eq. 1.[22]

$$4\ NH_2OH \longrightarrow 2\ NH_3 + N_2O + 3\ H_2O \qquad (1)$$

Despite N_2H_4 being more basic than NH_2OH by ca. 2 pK_a units,[23] we anticipated the Lewis acidity of the appended acid in **2-Br** to be of sufficient strength to independently capture NH_2OH, modelling the first step in cooperative activation. We tested this supposition by treating redox-inert $(^{BBN}NN^{tBu})ZnBr_2$

with NH_2OH in THF which produced $(^{BBN}NN^{tBu})ZnBr_2(NH_2OH)$ (**7**, Fig. 4).[24] Borane capture of NH_2OH was confirmed by IR and NMR spectroscopies. The ^1H NMR spectrum ($CDCl_3$) of **7** display B-NH_2 and –OH resonances at 7.01 and 4.98 ppm, respectively, while the and ^{11}B NMR spectrum indicated a tetrahedral boron centre at -2.94 ppm. The bonding metrics of both **6** and **7** were compared by examining their molecular structures obtained by XRD (Fig. 4, Table S21-S22). Compound **6** displays analogous bonding metrics to **4** with a B-NH_3 distance of 1.661(4) Å. Hydroxylamine complex **7** is the first structural example of a boron-hydroxylamine interaction and displays B-NH_2OH and N-O bond distances of 1.633(5) and 1.430(4) Å, respectively—each are equivalent to their N_2H_4 counterpart in $(^{BBN}NN^{tBu})ZnBr_2(N_2H_4)$. Isolation of **7** confirms the Lewis acidity requirement to capture NH_2OH is satisfied.

The reaction dichotomy in this system between N_2H_4 and NH_2OH (capture/reduction vs. disproportionation) can be rationalized by considering the relative stability of the anhydrous NH_2EH_x units versus their acid/base binding affinities. In the secondary coordination sphere, B-N bond formation is reversible for N_2H_4 and is likely more facile for NH_2OH due to its weaker basicity. Only an unquenched NH_2-lone-pair in NH_2OH can facilitate tautomerization to transient ammonia oxide, a proposed intermediate in NH_2OH decomposition.[25] Finally, H_2O always accompanies reactions with NH_2OH (50% v/v) and H_2O molecules have been found to participate in hydroxylamine decomposition via proton-transfer processes.[26] The fact that **2-Br** is not a N_2H_4 disproportionation catalyst enabled us to probe the homolytic bond scission pathway for that substrate — a reaction not yet possible for NH_2OH due to its propensity for disproportionation. In fact, controlled N-O bond homolysis of NH_2OH has not been demonstrated within a synthetic system. We are currently evaluating acidity and distance relationships to gain insight into N-N and N-O bond homolyses.

This work was supported by the NIH (1R01GM111486-01A1). N.K.S. is a Camille Dreyfus Teacher-Scholar. J.J.K. is supported by the NIH NIGMS F32GM126635. The authors thank Illinois St. Univ. for access to their diffractometer for data collection for **2-Br**. X-ray diffractometers were funded by the NSF (CHE 1625543, Purdue Univ.; CHE 1039689 Illinois St. Univ.).

Conflicts of interest

There are no conflicts to declare.

Notes and references

1. (a) Sippel, D.; Rohde, M.; Netzer, J.; Trncik, C.; Gies, J.; Grunau, K.; Djurdjevic, I.; Decamps, L.; Andrade, S. L. A.; Einsle, O., *Science* **2018,** *359*, 1484-1489; (b) Spatzal, T.; Aksoyoglu, M.; Zhang, L.; Andrade, S. L. A.; Schleicher, E.; Weber, S.; Rees, D. C.; Einsle, O., *Science* **2011,** *334*, 940-940; (c) Lancaster, K. M.; Roemelt, M.; Ettenhuber, P.; Hu, Y.; Ribbe, M. W.; Neese, F.; Bergmann, U.; DeBeer, S., *Science* **2011,** *334*, 974-977; (d) Hoffman, B. M.; Lukoyanov, D.; Dean, D. R.; Seefeldt, L. C., *Acc. Chem. Res.* **2013,** *46*, 587-595; (e) Hoffman, B. M.; Dean, D. R.; Seefeldt, L. C., *Acc. Chem. Res.* **2009,** *42*, 609-619; (f) Hoffman, B. M.; Lukoyanov, D.; Yang, Z.-Y.; Dean, D. R.; Seefeldt, L. C., *Chem. Rev.* **2014,** *114*, 4041-4062; (g) Hoeke, V.; Tociu, L.; Case, D. A.; Seefeldt, L. C.; Raugei, S.; Hoffman, B. M., *J. Am. Chem. Soc.* **2019**.
2. Vaughn, S. A.; Burgess, B. K., *Biochemistry* **1989,** *28*, 419-424.
3. Shaw, S.; Lukoyanov, D.; Danyal, K.; Dean, D. R.; Hoffman, B. M.; Seefeldt, L. C., *J. Am. Chem. Soc.* **2014,** *136*, 12776-12783.
4. Following sulphide ejection from the Fe-S cluster, a possible mechanism may involve N_2H_4/NH_2OH capture by a Lewis acidic Fe that positions the substrate for reduction by an adjacent Fe.
5. (a) Geri, J. B.; Shanahan, J. P.; Szymczak, N. K., *J. Am. Chem. Soc.* **2017,** *139*, 5952-5956; (b) Dahl, E. W.; Kiernicki, J. J.; Zeller, M.; Szymczak, N. K., *J. Am. Chem. Soc.* **2018,** *140*, 10075-10079; (c) Kiernicki, J. J.; Shanahan, J. P.; Zeller, M.; Szymczak, N. K., *Chem. Sci.* **2019,** *10*, 5539-5545; (d) Shanahan, J. P.; Szymczak, N. K., *J. Am. Chem. Soc.* **2019,** *141*, 8550-8556.
6. (a) Tutusaus, O.; Ni, C.; Szymczak, N. K., *J. Am. Chem. Soc.* **2013,** *135*, 3403-3406; (b) Kiernicki, J. J.; Zeller, M.; Szymczak, N. K., *J. Am. Chem. Soc.* **2017,** *139*, 18194-18197; (c) Kiernicki, J. J.; Zeller, M.; Szymczak, N. K., *Inorg. Chem.* **2019,** *58*, 1147-1154.
7. Polezhaev, A. V.; Chen, C.-H.; Losovyj, Y.; Caulton, K. G., *Chem. Euro. J.* **2017,** *23*, 8039-8050.
8. Tseng, K.-N. T.; Kampf, J. W.; Szymczak, N. K., *J. Am. Chem. Soc.* **2016,** *138*, 10378-10381.
9. Yang, L.; Powell, D. R.; Houser, R. P., *Dalton Trans.* **2007**, 955-964.
10. The reduction wave of **1-X** is irreversible while that of **2-X** is reversible presumably due to an irreversible reaction of the allyl fragment upon reduction of iron, see ESI for full analysis.
11. Steiner, T., *Angew. Chem. Int. Ed.* **2002,** *41*, 48-76.
12. Complex **3** shows similar intramolecular NH_2-Br hydrogen bonding interactions (ave. = 3.496 Å) as complex **4**.
13. Chen, C.-H.; Gabbaï, F. P., *Chem. Sci.* **2018,** *9*, 6210-6218.
14. Reversibiliy increases with faster scan rates, see ESI.
15. (a) Schmidt, E. W., *Hydrazine and Its Derivatives: Preparation, Properties, Applications*. 2nd ed.; John Wiley & Sons, Inc.: 2001; (b) Umehara, K.; Kuwata, S.; Ikariya, T., *J. Am. Chem. Soc.* **2013,** *135*, 6754-6757.
16. Yoo, C.; Lee, Y., *Angew. Chem. Int. Ed.* **2017,** *56*, 9502-9506.
17. Wickramasinghe, L. A.; Ogawa, T.; Schrock, R. R.; Müller, P., *J. Am. Chem. Soc.* **2017,** *139*, 9132-9135.
18. In the absence of reductant, **4** did not produce NH_4^+, while authentic samples of **5-Br** produced 0.87 equiv NH_4^+ (see ESI).
19. The 1,1-disubstituted hydrazines were not observed to interact with the trialkylborane at room temperature, see ESI.
20. (a) Bari, S. E.; Amorebieta, V. T.; Gutiérrez, M. M.; Olabe, J. A.; Doctorovich, F., *J. Inorg. Biochem.* **2010,** *104*, 30-36; (b) Bányai, I.; Dózsa, L.; Beck, M. T.; Gyémánt, G., *J. Coord. Chem.* **1996,** *37*, 257-270; (c) Alluisetti, G. E.; Almaraz, A. E.; Amorebieta, V. T.; Doctorovich, F.; Olabe, J. A., *J. Am. Chem. Soc.* **2004,** *126*, 13432-13442.
21. **2-Br** is stable to excess H_2O, but decomposes when exposed to excess NH_3, see ESI.
22. Under similar conditions, $(^{butyl}NN^{tBu})FeBr_2$ and $FeBr_2$ are NH_2OH disproportionation catalysts, see ESI.
23. Hall, H. K., *J. Am. Chem. Soc.* **1957,** *79*, 5441-5444.
24. Degradation of **7** is observed to procede via formal loss of H_2O. See ESI for X-ray structure.
25. Wang, Q.; Wei, C.; Pérez, L. M.; Rogers, W. J.; Hall, M. B.; Mannan, M. S., *J. Phys. Chem. A* **2010,** *114*, 9262-9269.
26. Wei, C.; Rogers, W. J.; Mannan, M. S., *Chem. Eng. Commun.* **2007,** *194*, 579-585.

Graphical Abstract

Tetrahedral Iron Featuring an Appended Lewis Acid: Distinct Pathways for the Reduction of Hydroxylamine and Hydrazine

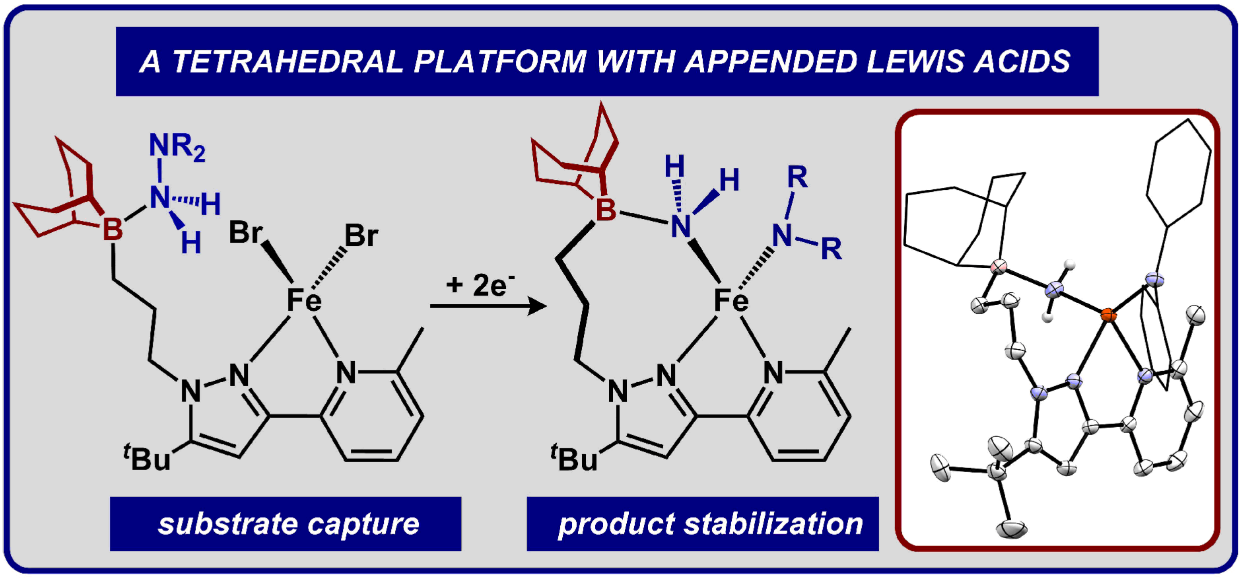

A tetrahedral iron complex bearing an appended Lewis acid is capable of effecting hydrazine and hydroxylamine reduction.